PERGAMON

RAPID SOLUTION HARDENING AT ELEVATED TEMPERATURES BY SUBSTITUTIONAL Re ALLOYING IN MoSi$_2$

A. MISRA†, A. A. SHARIF, J. J. PETROVIC and T. E. MITCHELL

Materials Science and Technology Division, Los Alamos National Laboratory, MS K765, Los Alamos, NM 87545, USA

Abstract—The mechanical properties of solidification processed polycrystalline MoSi$_2$ and ternary (Mo, Re)Si$_2$ alloys were evaluated by compression testing at elevated temperatures. Rhenium is found to be a potent solid solution hardening addition to C11$_b$ MoSi$_2$ at temperatures up to 1600°C (highest temperature used in the study). Dislocation microstructures, characterized by electron microscopy, are consistent with the significant hardening exhibited by Re containing alloys. The high hardening rate cannot be explained by the classical substitutional solid solution hardening theories for metals based on atomic size misfit and elastic moduli mismatch. Since rhenium "disilicide" is semiconducting and has a Si-deficient stoichiometry of ReSi$_{1.75}$, the addition of Re to MoSi$_2$ may lead to the formation of constitutional Si vacancies which may pair with Re substitutionals to form point defect complexes. A model that describes the elliptical strain field (tetragonal distortion) around these point defects is used to interpret the rapid hardening by Re in MoSi$_2$. Small additions of Re may provide the necessary high temperature strength in MoSi$_2$-based structural intermetallic alloys for very high temperature applications (~1200–1600°C). © 2000 Acta Metallurgica Inc. Published by Elsevier Science Ltd. All rights reserved.

Keywords: Intermetallics; High temperature; Dislocations; Transmission electron microscopy (TEM); MoSi$_2$

1. INTRODUCTION

MoSi$_2$ is a potential material for high temperature structural applications primarily due to its high melting point (2020°C), lower density (6.3 g/cm^3) compared with superalloys, excellent oxidation resistance, high thermal conductivity, and thermodynamic compatibility with many ceramic reinforcements [1–3]. However, low fracture toughness at near-ambient temperatures, low strength at elevated temperatures (> 1300°C) in the monolithic form and tendency to "pest" degradation at ~500°C have seriously limited the development of MoSi$_2$-based structural materials. Several recent studies have attempted to address these issues and have shown promising results. For example, pest resistant MoSi$_2$-based materials have been developed using silicon nitride reinforcement [4] or alloying with Al [5].

Deformation studies, in compression, on MoSi$_2$ single crystals have revealed a variety of slip systems [6]. For the body-centered tetragonal C11$_b$ structure of MoSi$_2$ shown in Fig. 1, the slip systems observed were:{013}⟨100]‡, {110}1/2⟨111], {011}⟨100] and {013}1/2⟨331] [6]. Furthermore, in single crystals with orientations other than [001], compressive plasticity has been reported at temperatures as low as −100°C [7, 8]. For the [001] orientation, only the {013}1/2⟨331] slip system is observed [6–8]. Due to the high critical resolved shear stress of this slip system as compared with systems with ⟨100] or 1/2⟨111] Burgers vector, compressive plasticity in [001] crystals has only been observed at temperatures > 900°C [6–8]. In addition to the slip systems reported by Maloy *et al.* [6], the {010}⟨100] and {023}⟨100] slip systems were also observed by Ito *et al.* [7, 8]. However, the primary slip vectors observed in single crystal studies are 1/2⟨111], ⟨100] and 1/2⟨331]. In polycrystals, generally only 1/2⟨111] and ⟨100] are observed and these account for only four independent slip systems [9]. For general polycrystalline ductility, five independent deformation modes are necessary [10, 11]. Changing the critical resolved shear stress of the slip systems

---

† To whom all correspondence should be addressed.

‡ The mixed notation {*hkl*} and ⟨*uvw*] is used to differentiate the first two indices from the third for the tetragonal crystal structure.

through alloying may be a way to activate all three slip vectors, (1/2⟨111], ⟨100] and 1/2⟨331]), and obtain polycrystalline ductility. In fact, solid solution softening has been observed at room temperature in $MoSi_2$ alloyed with Al [12, 13] and transition metals such as Nb, V and Ta [13]. The mechanism of softening is not clearly understood, although first principles calculations [14] indicate that solutes such as Al, Mg, V and Nb may change the Peierls stress so as to enhance {013)1/2⟨331] slip relative to cleavage. Clearly, more work is needed to understand how alloying may influence the mechanical behavior of $MoSi_2$.

With regard to elevated temperature strengthening of $MoSi_2$, both alloying with W to form $C11_b$ $(Mo, W)Si_2$ alloys and composites with ceramic reinforcements such as SiC have been tried. A $(Mo, W)Si_2/20$ vol.% SiC composite was shown to have significantly higher strength than Mar-M247 superalloy at temperatures above $1000°C$ [15]. However, the strength of the $(Mo, W)Si_2/20$ vol.% SiC composite dropped by almost an order of magnitude from 1200 to $1500°C$; the yield strength at $1500°C$ was only ~ 75 MPa [15]. A simpler and more effective way of strengthening $MoSi_2$ at elevated temperatures is needed where the strength can be better retained with increasing temperature above $1200°C$. Our preliminary studies using hot hardness experiments have shown that Re addition to $MoSi_2$ caused significant hardening up to $1300°C$ [16]. Further, it has been reported that alloying with Re, perhaps in synergism with carbon, increased the pesting resistance in the temperature range of $500–800°C$ [17]. In another preliminary study [18], polycrystalline $(Mo, Re)Si_2$ alloys exhibited a minimum creep rate of $\sim 5 \times 10^{-6}/s$ at 100 MPa applied stress at $1400°C$ as compared with the $1 \times 10^{-4}/s$ creep rate exhibited by $MoSi_2$. No detailed mechanistic study has been performed to understand the effects of Re alloying on the elevated temperature mechanical behavior of $MoSi_2$.

In the present investigation, we have evaluated the mechanical properties, in compression, of arc-melted polycrystalline $MoSi_2$ and $(Mo, Re)Si_2$ alloys. We find that significant strengthening is achieved up to $1600°C$ by only small additions of Re. The mechanisms of elevated temperature solid solution strengthening are elucidated by considering the generation of constitutional Si vacancies that may pair with Re substitutionals to form "tetragonally" distorted point defect complexes.

2. EXPERIMENTAL

$(Mo, Re)Si_2$ and $MoSi_2$ alloys were prepared by arc-melting elemental Mo, Re and Si with nominal 99.99% purity in an argon atmosphere. The buttons were turned over and remelted three to four times to ensure homogeneity. Rectangular parallelepipeds with dimensions $2 \times 2 \times 3$ mm^3 were cut from the arc-melted buttons. The samples were polished with SiC paper to 1 μm and finished with 0.05 μm colloidal silica. A series of $(Mo, Re)Si_2$ alloys of different compositions was used to determine the dependence of hardness on composition at room temperature. Compression testing as a function of temperature was performed only on the $(Mo_{0.925}Re_{0.075})Si_2$ alloy. All hardness and compression experiments were performed on polycrystalline materials. Compression testing was performed in air in the temperature range of 25–$1600°C$ at an initial strain rate of $\sim 1 \times 10^{-4}/s$. Thin foils for transmission electron microscopy (TEM) were prepared from the deformed materials by ion-milling. TEM was performed on a Philips CM30 operated at 300 kV.

3. RESULTS

3.1. Microstructures

The arc-melted materials studied had large grain sizes in the range of 100–150 μm. Impurities at grain boundaries, such as amorphous silica in hot pressed materials [19], were not found in solidification processed materials. In the $(Mo_{1-x}Re_x)Si_2$ alloys, for $x > \sim 0.25$, $ReSi_{2-x}$ and free Si phases were observed in addition to the $C11_b$ $(Mo, Re)Si_2$ phase and hence, the compression testing was performed only on low-Re alloys with ~ 2.5 at.% Re (i.e. $x = 0.075$).

3.2. Mechanical behavior

In our preliminary studies, published elsewhere [16], we found that rhenium "disilicide" actually had a Si-deficient stoichiometry of Re_4Si_7 and was much harder than $MoSi_2$—almost twice as hard at room temperature and more than three times as hard at $1300°C$. The ternary $(Mo_{0.925}Re_{0.075})Si_2$ alloy had intermediate hardness values at all temperatures and the results showed that Re is a potent solution hardener. Addition of 2.5 at.% Re
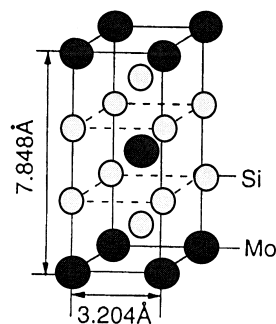

Fig. 1. Unit cell of the body-centered tetragonal $C11_b$ structure of $MoSi_2$.

increases the hardness of $MoSi_2$ by 30% at room temperature and 100% at 1300°C [16]. The results of the compression tests performed in this investigation are shown in Fig. 2(a) for $MoSi_2$ and in Fig. 2(b) for $MoSi_2 + 2.5$ at.% Re. In these graphs, an arrow at the end of the curve indicates catastrophic failure of the specimen. The stress–strain curves shown without an arrow at the end represent tests that were stopped prior to fracture. The minimum temperature at which measurable compressive plastic strain was noted was 900°C for $MoSi_2$, and 1000°C for $MoSi_2 + 2.5$ at.% Re. Our data for unalloyed polycrystalline $MoSi_2$ are consistent with those of Chang and Gibala [20] who observed compressive plasticity only at temperatures ≥ 900°C. In the temperature range of 750–850°C, modest compressive plasticity was only observed if $MoSi_2$ was pre-strained at 1300°C [20]. As shown in Fig. 2(a), arc-melted $MoSi_2$ can be easily plastically deformed at temperatures > 900°C; however, the yield strength drops significantly with increasing temperature from ~ 225 MPa at 1100°C to ~ 20 MPa at 1600°C. In the $MoSi_2 + 2.5$ at.% Re alloy, compressive plasticity is observed only at temperatures

> 1000°C, indicating an increase in the ductile-to-brittle transition temperature by Re alloying.

The 0.2% offset yield strengths of the unalloyed and Re-alloyed $MoSi_2$ are compared in Fig. 3. Note that the addition of only 2.5 at.% Re, causes the strength at 1600°C to be an order of magnitude higher than unalloyed $MoSi_2$. For unalloyed $MoSi_2$ the yield strength drops by about an order of magnitude from 1200 to 1600°C, while for Re-alloyed material the drop is only a factor of three. Recently, Inui et al. [21] have also observed that Re is a potent solid solution hardening addition to single crystal $MoSi_2$ at temperatures > 1300°C. For example, in the temperature range of 1300–1500°C the yield strength of $(Mo_{0.97}Re_{0.03})Si_2$ alloy was comparable with that of $(Mo_{0.5}W_{0.5})Si_2$ for the same single crystal orientation [21]. Thus, the solution hardening rate by Re is more than an order of magnitude higher than that of W in $MoSi_2$, even at temperatures as high as 1500°C. The mechanism for such rapid hardening is discussed later in this article.

3.3. Dislocation substructures

Typical dislocation substructures after compressive deformation at 1400°C are shown in Fig. 4(a) for $MoSi_2$ and in Fig. 4(b) for $MoSi_2 + 2.5$ at.% Re alloys. Regular arrays of sub-grains are observed in $MoSi_2$ with few isolated dislocations. Only ⟨100] dislocations were observed. This is consistent with results of Maloy et al. [6] on non-[001] oriented single crystals where low angle boundaries and some free ⟨100] dislocations were noted after compressive deformation at 1200–1300°C. The substructure shown in Fig. 4(a) is consistent with a climb-controlled dislocation creep deformation mode at elevated temperature, similar to the class M behavior in pure metals [22, 23]. In other words, due to the extremely low yield stress of $MoSi_2$ at 1400°C, dislocation glide is very fast and so climb of dislocations past the substructural obstacles becomes the
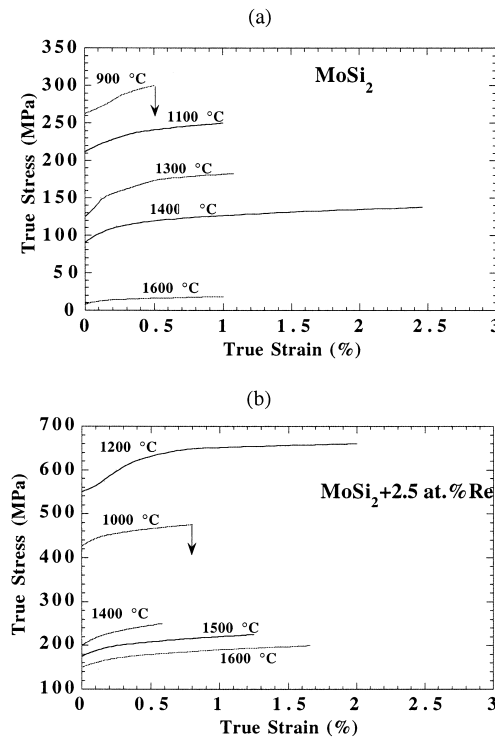

(a)

(b)

Fig. 2. Compressive stress–strain curves at different temperatures for (a) $MoSi_2$ and (b) $MoSi_2 + 2.5$ at.% Re alloys. In these graphs, an arrow at the end of the curve indicates catastrophic failure of the specimen. The stress–strain curves shown without an arrow at the end represent tests that were stopped prior to fracture.
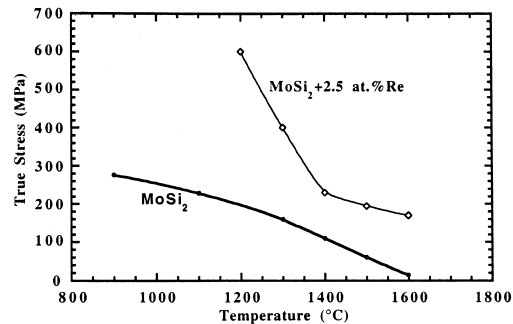

Fig. 3. Temperature dependence of 0.2% offset yield stress of $MoSi_2$ and $MoSi_2 + 2.5$ at.% Re alloys.

rate controlling factor. In contrast, addition of only 2.5 at.% Re changes the dislocation substructure significantly [Fig. 4(b)]. Here no significant tendency to form subgrains is noted and the dislocations are smoothly curved and randomly distributed. Such a substructure is consistent with class A or alloy behavior observed in disordered solid solutions [22, 23]. Thus, the addition of Re increases the flow stress and changes the elevated temperature behavior from climb-controlled to viscous glide-controlled where the glide of dislocation is restricted by the solute atoms. In creep tests, this change in the dislocation creep behavior by Re alloying would be further reflected in a decrease of the stress exponent from the pure metal behavior (≈ 5) to alloy behavior (≈ 3). Preliminary compressive creep testing by Chin *et al.* [18] for $MoSi_2$ and $(Mo, Re)Si_2$ alloys does show a lower dependence of minimum creep rate on applied stress in Re-alloyed materials. For example, for compressive creep at $1000°C$, the stress exponent changed from ≈ 4 for $MoSi_2$ to ≈ 2.3 for $(Mo, Re)Si_2$ [18].

For the substructure shown in Fig. 4(b), most of the dislocations have $\langle 100]$ Burgers vectors but some $1/2\langle 111 \rangle$ dislocations were also observed. For example, the dislocations labeled a, b and d in Fig. 4(b) have $\langle 100]$ Burgers vectors, and those labeled c and e are $1/2\langle 111 \rangle$ dislocation. The dissociation of $1/2\langle 111 \rangle$ dislocations was studied by weak beam imaging in the $(Mo, Re)Si_2$ alloy deformed at $1400°C$. A bright field image of $1/2\langle 111 \rangle$ dislocations for reflecting vector $\mathbf{g} = 006$ is shown in Fig. 5(a). For this imaging condition, all dislocations with $\langle 100]$ type Burgers vector are invisible. Weak beam images ($\mathbf{g}/3\mathbf{g}$ with $\mathbf{g} = 002$) of the non-screw dislocations labeled x and y in Fig. 5(a) are shown in Figs 5(b) and (c), respectively. Split dislo-
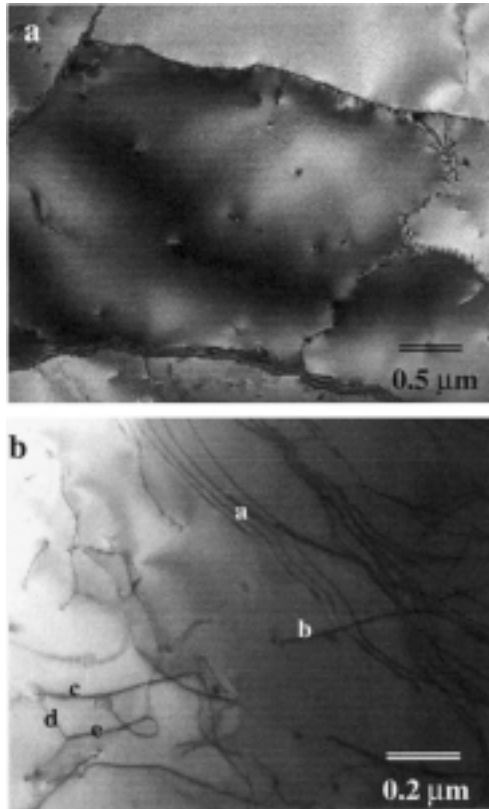
Fig. 4. Bright field TEM images showing the dislocation substructures in (a) $MoSi_2$ and (b) $MoSi_2 + 2.5$ at.% Re alloys deformed in compression at $1400°C$.
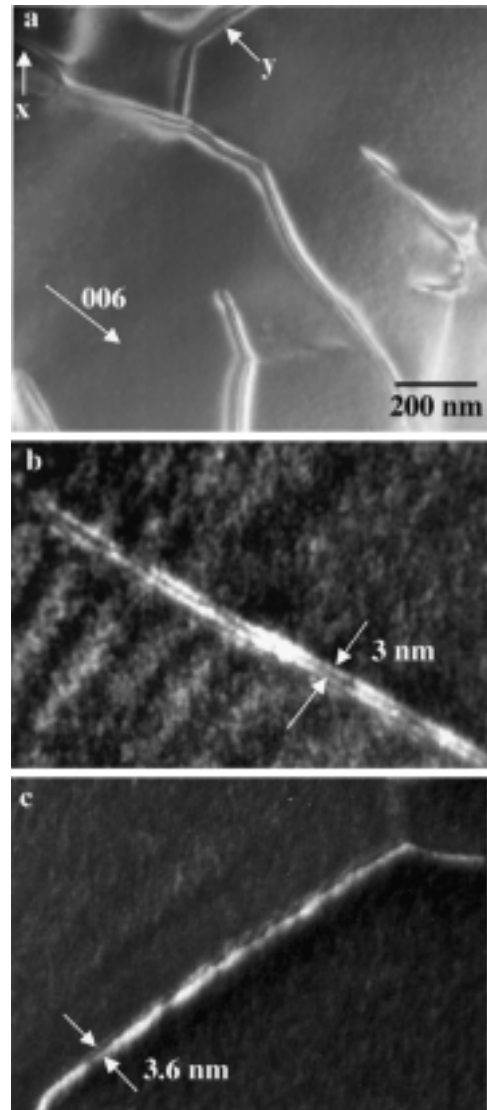

Fig. 5. (a) Bright field TEM image of $1/2\langle 111 \rangle$ dislocations in $MoSi_2 + 2.5$ at.% Re alloys deformed in compression at $1400°C$. Weak beam images of dislocations labeled x and y in (a) are shown in (b) and (c), respectively. The electron beam direction is ~ 5–$10°$ from [100].

cation images with separation of ~ 3 and ~ 3.6 nm are observed in Figs 5(b) and (c). The electron beam direction in these images was ~ 5–$10°$ from [100] towards [110]. Hence, the actual separation may be in the range of 4–5 nm if the dislocations are dissociated on the (110) slip plane. In unalloyed single crystal $MoSi_2$ deformed in compression at $1100°C$, $1/2\langle 111 \rangle$ dislocations were found to dissociate into $1/4\langle 111 \rangle$ partials [6, 7]. High-resolution imaging of the core revealed a planar core on the (110) slip plane [6]. The separation of the partials varied from ~ 4.4 nm for the screw orientation to ~ 6.8 nm for the $70°$ orientation [7]. For non-screw orientations, the separation was found to vary with orientation due to climb of the edge component. Our results indicate that Re alloying may increase the stacking fault energy associated with $1/2\langle 111 \rangle$ dislocations in $MoSi_2$.

4. DISCUSSION

The most striking result from this study is the significant elevated temperature strengthening, in compression, observed in $MoSi_2$ alloyed with Re. Even at $1600°C$, the yield strength of $MoSi_2 + 2.5$ at.% Re alloy is an order of magnitude higher than $MoSi_2$. Over the composition range where single phase $C11_b$ $(Mo, Re)Si_2$ alloys are observed, solid solution strengthening is the only reasonable mechanism by which the yield strength is increased with Re alloying. In an attempt to explain the observed strengthening, we first use the classical theories for solution hardening in metals.

4.1. Substitutional solid solution strengthening

Here we use the Fleischer model [24, 25] developed for solution strengthening in pure metals by substitutional solutes. The strengthening arises primarily due to (i) the shear modulus mismatch between the solute and the matrix atoms, and (ii) the atomic size misfit between the solute and the matrix. It is assumed that the stress field around a substitutional solute is spherically symmetric. The hardening from this mechanism is usually gradual with increasing concentration of solute. This is due to the fact that there is very weak or no interaction between screw dislocations that do not have a hydrostatic stress field around them and substitutional solutes with spherically symmetric volume misfit strain field. Fleischer [24] defined the size misfit (ε_a) and modulus misfit (ε_G') parameters as follows:

$$\varepsilon_a = \frac{1}{a}\left(\frac{\mathrm{d}a}{\mathrm{d}c}\right)$$

$$\varepsilon_G' = \frac{\varepsilon_G}{(1 + 0.5\varepsilon_G)}$$

where

$$\varepsilon_G = \frac{1}{G}\left(\frac{\mathrm{d}G}{\mathrm{d}c}\right).$$

In the above equations, $\mathrm{d}a/\mathrm{d}c$ and $\mathrm{d}G/\mathrm{d}c$ reflect the rate of change of lattice parameter (a) and shear modulus (G) of matrix with the solute concentration (c). These misfit strains were combined to give a Fleischer parameter, ε_s, defined as

$$\varepsilon_s = \left| \varepsilon_G' - \beta\varepsilon_a \right|$$

where $\beta = 3$ for screw dislocations and 16 for edge dislocations.

Hence, for a given substitutional solute and matrix combination, ε_s can be calculated if the dependence of G and a on c are known. The increase in shear strength ($\Delta\tau$) as a function of solute concentration is then given as follows [24]:

$$\Delta\tau = \frac{G\varepsilon_s^{3/2}c^{1/2}}{\alpha} \qquad (1)$$

where α is a material sensitive parameter. For substitutional solution hardening in f.c.c. metals, $\alpha \approx 700$. In order to test whether this model may be applicable, we plot the room temperature hardness of $(Mo, Re)Si_2$ alloys as a function of $\sqrt{c}$ where c is taken as the atomic fraction of Re in $MoSi_2$, following the approach used by Fleischer for analyzing solution hardening in B2 intermetallics [26]. The result is shown in Fig. 6. Note that the hardness scales linearly with $\sqrt{c}$ as predicted by equation (1). Thus, we can proceed to use equation (1) to calculate the value of α that would fit the experimental solution hardening data for $(Mo, Re)Si_2$ alloys. In our previous studies, we have determined the lattice parameters and elastic constants of $ReSi_2$ [27, 28]. We calculate $\mathrm{d}a/\mathrm{d}c$ and $\mathrm{d}G/\mathrm{d}c$ assuming linear interpolation between $MoSi_2$ and $ReSi_2$ for a and G. Using G for $MoSi_2$ as 192 GPa [27] and considering the screw dislocation case ($\beta = 3$), ε_s is calculated as 0.264. At $1200°C$, the increase in compressive yield
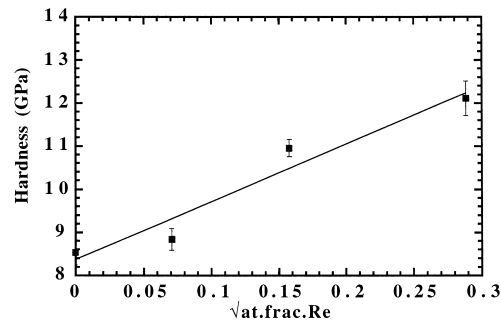
Fig. 6. Dependence of room temperature hardness of $(Mo, Re)Si_2$ alloys on square root of the Re concentration.

strength of $MoSi_2$ is 400 MPa for 2.5 at.% Re. Using a Taylor factor of 3, we obtain $\Delta\tau \approx 133$ MPa. Substitution of $\Delta\tau$, ε_s, c, and G in equation (1) gives $\alpha = 30$. Similarly, using hardness values from Mitchell and Misra [16] and assuming that hardness is a factor of three higher than compressive yield strength, we obtain $\alpha = 25$ at 1200°C and $\alpha = 15$ at room temperature. Thus, the rate of hardening by Re in $MoSi_2$, i.e. α in equation (1) is on the order of 15–30. It is well known that in metals $\alpha \approx 700$ for substitutional hardening [24]. The observed hardening rate is extremely rapid and cannot be treated within the framework of classical substitutional hardening theories for disordered metallic alloys. For B2 intermetallics such as CoAl, Fleischer has observed $\alpha \approx 250$ and argued that this is still consistent with the conventional substitutional hardening theory since intermetallics may have more complex unit cells and longer Burgers vectors than pure metals [26]. However, for Ti, Co and Fe alloying in RuAl, α was found to be in the range of 13–25 [26]. It was suggested that such rapid hardening could not be explained using the conventional model shown in equation (1).

In more recent studies, anomalous substitutional hardening in B2 intermetallics has been reported by several other investigators [29–31]. It is postulated that substitutional alloying in intermetallics may lead to the formation of constitutional vacancies [29]. Furthermore, depending on the thermal history, the intermetallic alloys may contain quenched-in thermal vacancies [29–31]. Precise density measurements combined with lattice parameter measurements have been used to measure the vacancy concentration in B2 aluminides [29]. For thermal vacancies, vacancy concentration can only be obtained through such precise measurements. For constitutional vacancies, the point defect concentration is a linear function of the deviation from stoichiometry and can thus be calculated. We now explain how Re alloying in $MoSi_2$ may lead to formation of point defects and use a model to explain this anomalous strengthening.

4.2. Anomalous substitutional hardening through creation of point defects

Our recent investigations of the structure of $ReSi_2$ have revealed that this "disilicide" has a Si-deficient stoichiometry of $ReSi_{1.75}$ (or Re_4Si_7) [16, 27, 28]. Since "$ReSi_2$" is a semiconductor, it must have an even number of valence electrons per unit cell and the stoichiometry of Re_4Si_7 provides this. Hence, the ternary Mo–Re disilicides are really alloys in the composition field $MoSi_2$–Re_4Si_7 and not $MoSi_2$–$ReSi_2$. Thus, the stoichiometry of $MoSi_2 + 2.5$ at.% Re alloy should be expressed as $(MoSi_2)_{0.925}(ReSi_{1.75})_{0.075}$, rather than $(MoSi_2)_{0.925}(ReSi_2)_{0.075}$. It follows that the

stoichiometry of $MoSi_2 + 2.5$ at.% Re alloy is $(Mo_{0.925}Re_{0.075})Si_{1.98125}$, and from this we obtain the Si vacancy concentration, V_{Si}, of 0.00625 for this alloy (in other words, one Si vacancy for every four Re atoms). Thus, we can calculate V_{Si} for all the alloys and replot the data of Fig. 6 as room temperature hardness vs $\sqrt{V_{Si}}$ (shown in Fig. 7). A linear relationship is observed only with $\sqrt{V_{Si}}$ and not with V_{Si}, consistent with the observations of Pike *et al.* [29] on B2 aluminides. Thus, the room temperature rapid hardening may be linked with the constitutional vacancies that are created in $(Mo, Re)Si_2$ alloys. However, the strain field around an isolated vacancy may not have a tetragonal distortion as strong as that around an interstitial [32]. Hence, we believe that rapid hardening due to constitutional vacancies may require pairing of point defects to form complexes, e.g. Re substitutional atoms may pair with vacancies. The stress field around these defect complexes will be significantly more tetragonally distorted as compared with isolated Re substitutional atoms or Si vacancies. Furthermore, we note that strengthening by Re is observed at elevated temperatures as well. At temperatures as high as 1600°C, the isolated constitutional vacancies may be expected to make dislocation creep easy, thereby reducing or completely eliminating the strengthening effect due to Re. Thus strengthening at high temperatures may only be possible if the Si vacancies pair with the Re substitutional atoms to form defect complexes.

With regard to the nature of point defects responsible for strengthening, we believe that constitutional vacancies in $(Mo, Re)Si_2$ alloys dominate and the role of thermal vacancies generated during testing may be ignored. In other intermetallics such as FeAl, a thermal-vacancy hardening model has been used to explain the yield strength anomaly [31]. According to this model, the anomalous increase in yield strength with increasing temperature may be due to increased vacancy hardening since the concentration of thermal vacancies increases with increasing temperature [31]. Above a
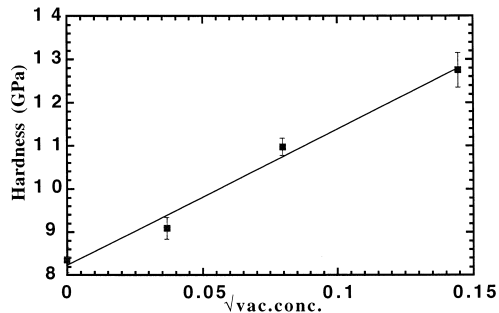

Fig. 7. Dependence of room temperature hardness of $(Mo, Re)Si_2$ alloys on square root of the Si vacancy concentration.

critical temperature (and hence, a critical vacancy concentration), the excess vacancies may accelerate dislocation creep making plastic flow easier. These two competing mechanisms result in a peak in the yield stress vs temperature curve [31]. In our case significant strengthening is observed well above the peak temperature of the flow stress anomaly (~ 800–900°C) of unalloyed $MoSi_2$. Hence, we focus only on constitutional vacancies and, in order to explain rapid hardening at all temperatures, we use the hypothesis that point defect complexes form between Si vacancies and Re substitutional atoms.

Anomalous solution hardening has also been reported in ionic crystals upon substitutional alloying with aliovalent cations [33]. For example, in MgO the solution hardening rate due to Fe^{3+} is an order of magnitude greater than that due to Fe^{2+} [34]. It is generally accepted that this effect is due to the complexes formed by the aliovalent cations with their charge compensating defects that can either be vacancies or interstitials [33]. Such a paired defect complex will cause both an elastic and an electrostatic distortion of the lattice; however, the elastic distortion was found to be the dominant factor [33]. Similarly, the constitutional vacancies formed in $MoSi_2$–Re_4Si_7 alloys may pair with the Re substitutional atoms to neutralize the extra electron carried by the Re atom. The detailed structure of the point defect complexes that form is unclear. Two possible defect complexes are shown schematically in Fig. 8. A Si vacancy may pair with a Re substitutional atom to form a strain dipole [Fig. 8(a)]. Alternatively, since the stoichiometry of rhenium "disilicide" is Re_4Si_7, one Si vacancy is expected for every four Re substitutional atoms; hence, four Re atoms may cluster around a Si vacancy as shown in Fig. 8(b). Since the number of valence electrons in Mo atoms is six and in Re atoms is seven, Re atoms increase the electron-to-atom (e/a) ratio of

Fig. 8. Schematic of the paired Re substitutional atom and Si vacancy point defect complex in $MoSi_2$–Re_4Si_7 alloys: (a) one Re substitutional atom paired with one Si vacancy shown in a [100] projection; (b) four Re substitutional atoms paired with one Si vacancy shown in a [001] projection. The unit cells in both projections are indicated by dotted lines. The elastic strain field caused by these defect complexes is elliptical rather than spherically symmetric as around a substitutional solute.

$MoSi_2$. The pairing of Si vacancies with Re atoms will locally reduce the e/a ratio, similar to the pairing of aliovalent cations with charge compensating point defects in ceramics. The strain field around this point defect complex will be elliptical (tetragonal distortion) rather than spherically symmetric as around substitutional solutes. Thus, the strengthening obtained will change significantly since dislocations will interact differently with these defects.

The interaction of dislocations with the elastic strain field of such defects has been modeled by Mitchell and Heuer [33] using anisotropic elasticity for cubic crystals and Friedel statistics (localized interactions between point defects and dislocations). The Mitchell–Heuer model is as follows:

$$\Delta\tau = \left(\frac{1.25\Omega_d}{4\pi\Omega^{1/3}\lambda^2}\right)^{3/2}\left(\frac{\beta d}{b}\right)^{1/2}\left(\frac{M^3\alpha^{3/2}}{\gamma}\right)^{1/2}\Delta\varepsilon^{3/2}GV_{Si}^{1/2}$$

(2)

where $\Delta\tau$ is the increase in the shear stress, Ω_d is the volume of the defect complex, Ω is the atomic volume per substitutional, λ is the perpendicular distance between the dislocation glide plane and the center of the tetragonal distortion, $\beta = 2/3$ for screw and 1 for edge dislocations, d is the separation between an aliovalent cation and its charge compensating defect, $M = 1/(1-\upsilon)$ for isotropic, $\alpha = (C_{11} - C_{12})/2C_{44}$ is the anisotropy factor, $\gamma = \Gamma/Gb^2$ where Γ is the line tension and b is the Burgers vector, and $\Delta\varepsilon$ is the "tetragonality" of the complex, i.e. the difference between the strain along the major and the minor axes of the elliptical strain field. For spherically symmetric distortion, $\Delta\varepsilon = 0$. The $\Delta\tau \propto \Delta\varepsilon^{3/2}$ dependence results from Friedel statistics; using Mott statistics for diffuse interactions between solute and dislocation would result in $\Delta\tau \propto \Delta\varepsilon$ dependence [33].

To use this model, all factors are either known or can be approximated knowing the lattice and elastic constants except for $\Delta\varepsilon$. Hence, we fit the model to the strengthening data at 1200°C and obtain $\Delta\varepsilon$. We have assumed $\Omega_d = \Omega = b^3$, $d = \lambda = b$, $\beta = 2/3$, $\alpha = 1$, $\upsilon = 0.151$ and a Taylor factor of three to convert shear stress to uniaxial stress. For 2.5 at.% Re, V_{Si} is shown in Fig. 7. We thus obtain $\Delta\varepsilon = 0.27$. In other words, for an elliptical strain field around this defect complex, the difference in strain along the major axis and the minor axis is 0.27. Since there is no direct way to measure $\Delta\varepsilon$, we compare the value with other cases of tetragonal distortions. The most common example of rapid solution hardening is due to interstitials, either impurities or self-interstitials [25]. For carbon in Fe, $\Delta\varepsilon$ is 0.41 [35]; for interstitial Cu atoms in Cu, the calculated value of $\Delta\varepsilon$ is 0.55 [36, 37]. For the different ionic crystals studied by Mitchell and Heuer [33], $\Delta\varepsilon$ values ranged from 0.07 to 0.57 depending on the material and temperature. Hence, we conclude that
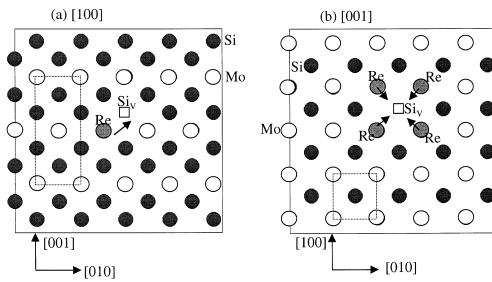
our calculated value of $\Delta\varepsilon = 0.27$ is consistent with the "tetragonality" observed in other investigations of rapid solution hardening. Of course, more work is needed using positron annihilation spectroscopy to determine the concentrations of vacancies in our alloys. Also, creep testing is needed over a range of temperatures and stresses to fully assess the effect of Re alloying on the elevated temperature strengthening of $MoSi_2$. Nevertheless, this work has identified that small additions of Re can significantly enhance the high temperature strength of $MoSi_2$. However, the room temperature toughness of $(Mo, Re)Si_2$ alloys is comparable with $MoSi_2$ [16]. Recent studies have shown that elements such as Al and Nb in small amounts (1–2 at.%) can lower the room temperature hardness and enhance plasticity of $MoSi_2$, without significantly affecting the elevated temperature strength [12, 13]. Hence, it may be possible to develop quaternary $(Mo, Re)(Si, Al)_2$ alloys with higher elevated temperature strength and higher room temperature ductility as compared with $MoSi_2$. The structure and properties of these quaternary alloys are currently being studied in our lab and will be published later.

5. SUMMARY

We have observed that small additions of Re (≤ 2.5 at.%) cause a significant increase in the compressive yield strength of polycrystalline $MoSi_2$ up to a temperature of 1600°C. This rapid solution hardening cannot be explained using the conventional Fleischer model of substitutional solution hardening assuming a spherically symmetric strain field around solutes. Since the stoichiometry of "$ReSi_2$" is in fact $ReSi_{1.75}$, the $MoSi_2$–$ReSi_{1.75}$ "disilicide" alloys will actually be Si-deficient and contain constitutional vacancies. Since Re has a higher electron-to-atom ratio than Mo, we postulate that Si vacancies may act as charge compensating defects and pair with Re substitutionals to create point defect complexes. The rapid hardening can then be attributed to the elliptical strain field around these point defect complexes, following the Mitchell–Heuer model originally developed for ionic crystals.

REFERENCES

1. Petrovic, J. J., *Ceram. Engng Sci. Proc.*, 1997, **18**, 3.
2. Mitchell, T. E., Castro, R. G., Petrovic, J. J., Maloy, S. A., Unal, O. and Chadwick, M. M., *Mater. Sci. Engng*, 1992, **A155**, 241.
3. Gibala, R., Ghosh, A. K., Van Aken, D. C., Srolovitz, D. J., Basu, A., Chang, H., Mason, D. P. and Yang, W., *Mater. Sci. Engng*, 1992, **A155**, 147.
4. Hebsur, M. G. and Nathal, M. V., in *Structural Intermetallics 1997*, ed. M. V. Nathal, *et al.* The Minerals, Metals and Materials Society, Warrendale, PA, 1997, p. 949.
5. Stergiou, A. and Tsakiropoulos, P., in *Structural Intermetallics 1997*, ed. M. V. Nathal, *et al.* The Minerals, Metals and Materials Society, Warrendale, PA, 1997, p. 869.
6. Maloy, S. A., Mitchell, T. E. and Heuer, A. H., *Acta metall. mater.*, 1995, **43**, 657.
7. Ito, K., Inui, H., Shirai, Y. and Yamaguchi, M., *Phil. Mag. A*, 1995, **72**, 1075.
8. Ito, K., Yano, T., Nakamoto, T., Moriwaki, M., Inui, H. and Yamaguchi, M., *Prog. Mater. Sci.*, 1997, **42**, 193.
9. Maloy, S. A., Heuer, A. H., Lewandowski, J. J. and Mitchell, T. E., *Acta metall. mater.*, 1992, **40**, 3159.
10. von Mises, R., *Z. angew. Math. Mech.*, 1928, **8**, 161.
11. Groves, G. W. and Kelly, A., *Phil. Mag.*, 1963, **8**, 877.
12. Peralta, P., Maloy, S. A., Chu, F., Petrovic, J. J. and Mitchell, T. E., *Scripta mater.*, 1997, **37**, 1599.
13. Harada, Y., Murata, Y. and Morinaga, M., *Intermetallics*, 1998, **6**, 529.
14. Waghmare, U. V., Bulatov, V., Kaxiras, E. and Duesbery, M. S., *Mater. Sci. Engng*, 1999, **261A**, 147.
15. Vasudevan, A. K. and Petrovic, J. J., *Mater. Sci. Engng*, 1992, **155A**, 1.
16. Mitchell, T. E. and Misra, A., *Mater. Sci. Engng*, 1999, **261A**, 106.
17. Davidson, D. L. and Bose, A., *Mater. Res. Soc. Symp. Proc.*, 1994, **322**, 431.
18. Chin, S., Anton, D. L. and Giamei, A. F., Annual Technical Report R94-970281-2, United Technologies Research Center, East Hartford, CT, 1994.
19. Aikin Jr, R. M., *Scripta metall.*, 1992, **26**, 1025.
20. Chang, H. and Gibala, R., *Mater. Res. Soc. Symp. Proc.*, 1994, **322**, 223.
21. Inui, H., Ishikawa, K. and Yamaguchi, M., *Proceedings of the US–Japan Workshop on "Very High Temperature Structural Materials"*, Turtle Bay, Hawai, 9–11 December 1998.
22. Mohamed, F. A. and Langdon, T. G., *Acta metall.*, 1974, **22**, 779.
23. Soliman, M. S. and Mohamed, F. A., *Mater. Sci. Engng A*, 1982, **55**, 111.
24. Fleischer, R. L., *Acta metall.*, 1963, **11**, 203.
25. Fleischer, R. L., in *The Strengthening of Metals*, ed. D. Peckner. Reinhold Press, New York, 1964, pp. 93–162.
26. Fleischer, R. L., *Acta metall.*, 1993, **41**, 1197.
27. Misra, A., Chu, F. and Mitchell, T. E., *Scripta mater.*, 1998, **38**, 917.
28. Misra, A., Chu, F. and Mitchell, T. E., *Phil. Mag. A*, 1999, **79**, 1411.
29. Pike, L. M., Chang, Y. A. and Liu, C. T., *Acta mater.*, 1997, **45**, 3709.
30. Schneibel, J. H., Specht, E. D. and Simpson, W. A., *Intermetallics*, 1996, **4**, 581.
31. George, E. P. and Baker, I., *Intermetallics*, 1998, **6**, 759.
32. Hirth, J. P. and Lothe, J., in *Theory of Dislocations*. John Wiley, New York, 1982, p. 501.
33. Mitchell, T. E. and Heuer, A. H., *Mater. Sci. Engng*, 1977, **28**, 81.
34. Groves, G. W. and Fine, M. E., *J. appl. Phys.*, 1964, **35**, 3587.
35. Cochardt, A. W., Schoeck, G. and Wiedersich, H., *Acta metall.*, 1955, **3**, 533.
36. Gibson, J. B., Goland, A. N., Milgram, M. and Vineyard, G. H., *Phys. Rev.*, 1960, **120**, 1229.
37. Huntington, H. B., *Phys. Rev.*, 1953, **91**, 1092.